International Journal of Mass Spectrometry 278 (2008) 170–177

Contents lists available at ScienceDirect

International Journal of Mass Spectrometry

journal homepage: www.elsevier.com/locate/ijms

Development of a low power, high mass range mass spectrometer for Mars surface analysis

Theresa Evans-Nguyen[a], Luann Becker[b], Vladimir Doroshenko[c], Robert J. Cotter[a,*]

[a] Department of Pharmacology and Molecular Sciences, Johns Hopkins School of Medicine, Baltimore, MD 21205, United States
[b] Department of Physics and Astronomy, Johns Hopkins University, Baltimore, MD 21218, United States
[c] Mass Technologies, Inc., Columbia, MD 21046, United States

ARTICLE INFO

Article history:
Received 5 August 2008
Received in revised form 2 September 2008
Accepted 2 September 2008
Available online 10 September 2008

Keywords:
Quadrupole ion trap
Laser desorption
Electron ionization

ABSTRACT

A compact, low power quadrupole ion trap mass spectrometer is being developed that will achieve a mass range of 2000 Da at low voltage (0–300 V_{0-p}) using a lower frequency fundamental voltage and supplemental excitation to very low $q_{excitation}$ parameter. The instrument is a prototype for a spacecraft hardware design referred to as the Mars Organic Mass Analyzer (MOMA) that is currently scheduled for flight to Mars in 2013 as part of the European Space Agency ExoMars mission. MOMA is one of two "life detection" instruments that are being sponsored by NASA. MOMA will accommodate both an atmospheric pressure laser desorption ionization source that will provide direct sampling of core samples for the detection of organics over a broad mass range and an electron ionization source coupled to a gas chromatograph for the detection of atmospheric gases and specific biomarkers (e.g., amino acids, nucleobases, etc.). The instrument reported herein is an early prototype used to demonstrate the basic design concepts for a low power instrument with high mass range, including the use of supplemental frequency scans to record mass spectra. In addition, mass spectra are obtained using CO_2 (the major constituent of the Mars atmosphere) as the bath gas, and a novel internal electron ionization source has been developed in which the electron beam enters through the ring electrode.

1. Introduction

Mass spectrometers have now flown in several planetary exploration missions including the Viking missions to Mars [1,2], the Pioneer mission to Venus [3], and the Galileo [4] and Cassini [5] missions to Saturn. The magnetic sector analyzers of the Viking missions to Mars [6,7] utilized a permanent magnet system that required little power, though miniaturization did limit their mass range. The so-called neutral mass spectrometer (NMS) designed by Alfred O. Nier and launched August 20, 1975 was a double-focusing (electrostatic and magnetic) mass spectrometer used to measure the concentrations of species in the Mars atmosphere. It employed electron ionization and had two collectors monitoring the mass ranges 1–7 Da and 7–49 Da. The GCMS designed by Klaus Biemann and launched September 9, 1975 was designed to examine organics that evolved from heating soil samples to 600 °C with a mass range of 12–200 Da. Unfortunately the Viking GCMS did not detect any definitive organic compounds, likely due to the harsh environment (H_2O_2) and highly oxidizing conditions that characterize the Martian surface today [8,9]. However, the Viking NMS did make several key atmospheric measurements on the surface of Mars that have led to the discovery of some 2 dozen Martian meteorites on Earth. All of these meteorites contained glass inclusions with trapped gases (noble gases) that are identical to the atmospheric gases that NMS measured on the surface of Mars in 1976 [10]. Miniaturized quadrupoles were used in the ion/neutral mass spectrometer (INMS) in the orbiter launched in 1997 as part of the Cassini Mission to Saturn/Titan, and in the Huygens Probe aerosol pyrolyzer GCMS. The mass range on these instruments was from 1 Da to 99 Da. Several mass spectrometers are on board the Rosetta mission that will rendezvous with the comet Churyumov-Gerasimenko in 2014. The COSIMA (cometary dust secondary ion mass analyzer) is a TOF-SIMS instrument, and two sensors on the ROSINA (Rosetta orbiter spectrometer for ion and neutral analysis) include a reflectron TOF mass spectrometer and a quadrupole ion trap. The ion trap is of reduced size using low voltage (300 V), low frequency RF to achieve a mass range of around 150 Da. Recent and upcoming missions seeking more conclusive proof of life on Mars include the Phoenix TEGA mission [11] (recently landed on July 4), and the Mars Science Laboratory [12] (launch scheduled for 2009)—all of which employ mass spectrometers for their well-recognized sensitivity.

* Corresponding author. Tel.: +1 410 955 3022; fax: +1 410 955 3420.
E-mail address: rcotter@jhmi.edu (R.J. Cotter).

1387-3806/$ – see front matter © 2008 Published by Elsevier B.V.
doi:10.1016/j.ijms.2008.09.002

Table 1
Quadrupole and cylindrical ion trap parameters

Parameter	Finnigan	Cooks [20]	Rosetta [21]	Cylindrical [22]	MOMA
Fundamental $\omega/2\pi$ (MHz)	1.1	1.1	0.6	1.1	0.8
Maximum amplitude V_{max} (0–p)	7.5 kV	7.5 kV	300 V	7.5 kV	300 V
Radius, r_0 (cm)	1.0	0.5	0.8	1.0	0.5
Axis $2z_0$ (cm)	1.57	0.78	1.13	1.79	0.71
Mass range (Da) in *mass-selective instability* mode $q_{eject} = 0.908$	650	2,600	150	600	200
Supplemental RF frequency (kHz)	69.9	NA	NA	425	34.4
q_{eject}	0.182	NA	NA	NA	0.089
Mass range (Da) in *resonance ejection mode*	3,250	NA	NA	NA	2,000

The renewed interest in the exploration of extant or extinct life on Mars has emerged because of several factors including the recent discovery of water—critical to the theories of the origin of life [13]. Furthermore, analysis of the Martian meteorite ALH84001 revealed several polycyclic aromatic hydrocarbons [14] and carbonate nodules [15,16] dating back over 3.85 billion years, from a time in the geological record when life on Earth began [13]. Both current (the Mars Exploration Rovers or MRO, Phoenix) and future missions (Mars Science Laboratory, MSL ExoMars) have keyed on evidence of abundant water and water 'ice', an essential ingredient to life on Earth. Both MSL and ExoMars will concentrate on the detection of key biomarkers and organics to directly address whether or not life ever occurred on Mars.

For mass spectrometers aboard planetary missions, severe power and mass constraints are uncompromising. Because Mars has an atmosphere of 5–10 Torr, some form of pumping is required. The quadrupole ion trap is an attractive choice of mass analyzer because of its relative resilience to moderately high pressures but is, unfortunately, historically limited in mass range. The mass range of most space-flight mass spectrometers has in fact been limited to the study of small masses (<600 Da), with the exception of COSAC [17,18] which featured a TOF-MS (with a mass range of 5000 Da). However, it is the detection of high mass organic species (>1000 Da), such as the highly cross-linked organic polymers known as kerogens that would be indicative of life.

With mass range directly proportional to the fundamental RF amplitude, commercial traps reach voltages of 8500 V_{0-p} to achieve m/z ranges up to 2 kDa. In fact, 8500 V_{0-p} has been an upper limit due to dielectric breakdown. As is well characterized by the Mini-series of ion traps pioneered by Cooks and co-workers [19], RF power is of great concern and has prompted the movement to miniaturization which makes use of lower RF voltages in field portable ion trap instruments. To achieve a reasonable mass range under low power constraints, we are developing a low-voltage RF trap which makes use of resonance ejection for mass range extension, a relatively small r_0, and a low fundamental driving frequency to allow operation of the fundamental RF no higher than 500 V_{0-p}. Precedent for such an ion trap lies in the operation of the Ptolemy Comet Chaser GC–MS system [18]. The unique feature of our instrument is the addition of resonance ejection to such a low voltage instrument to achieve mass range extension beyond the 150 Da of Ptolemy.

In this report we describe the initial development of a low power quadrupole ion trap mass spectrometer for space flight specifically designed for the analysis of organic species on Mars using the Mars Organic Molecule Analyzer (MOMA). The ion trap was the instrument of choice for a number of reasons: (1) it could more conveniently be interfaced to an external (Mars) atmospheric ionization source, (2) it could provide the opportunity for carrying out MS/MS analyses and (3) most of its parameters are scalable, making it possible to achieve the target 2000 Da mass range using low voltage and low power. Specifically, in the *mass-selective instability mode* of operation (which uses only the fundamental frequency Ω applied to the ring electrode), the maximum mass that can be scanned out of the ion trap is:

$$(m/z)_{max} = \frac{4\,V_{max}e}{q_{eject}\Omega^2(r_0^2 + 2z_0^2)} \quad (1)$$

where V_{max} is the maximum amplitude of the fundamental RF voltage, r_0 is the inside radius of the ring electrode, z_0 is the distance from the trap center to endcap, and q_{eject} is the ejection parameter.

The commercial ion trap mass spectrometers developed by Finnigan Corporation (now Thermo, Sunnyvale, CA), utilize a fundamental RF frequency of 1.1 MHz at a maximum amplitude of 7.5 kV_{0-p} on a 1.0 cm trap to achieve a mass range (in the *mass selective instability* mode) of 650 Da (see column 2 in Table 1). The mass range is extended by the addition of a supplementary RF voltage on the trap endcaps; in the example below a supplemental RF frequency of 69.9 kHz shifts the ejection parameter (normally 0.908 in the *mass selective instability* mode) to $q_{eject} = 0.182$. In the so-called *resonance ejection mode* the amplitude of the fundamental RF is scanned in the same fashion up to 7.5 kV_{0-p}, but the mass range is extended to 3250 Da.

A number of other configurations, including the target configuration for the MOMA instrument, are also shown in Table 1. Cooks and co-workers [20] described a method for mass extension that utilized a 0.5 cm trap. Operated in the *mass selective instability* mode only, this resulted in a mass range of 2600 (column 3 in Table 1). The Rosetta mission (column 4) uses a low voltage (300 V_{0-p}) 600 kHz ion trap with $r_0 = 0.8$ cm, $2z_0 = 1.13$ cm to achieve a mass range of 150 [18]. While this is a considerably smaller mass range, it was compatible with the planned GCMS experiments and illustrates the use of the scalability of these parameters to achieve a low voltage, low power configuration for space applications. An interesting cylindrical geometry ion trap has also been described by Cooks and co-workers [22] having parameters and mass range (600 Da) similar to the commercial quadrupole traps (column 5). A supplemental voltage at relatively high frequency (425 kHz) does not produce an appreciable change in the ejection parameter, but allows the instrument to be scanned in the *resonance ejection mode*, producing better mass resolution. The target mass range for the MOMA mass spectrometer is 2000 Da using a low fundamental RF voltage. One set of parameters, using lowered frequency, smaller radius and a supplemental RF voltage to achieve a very low q_{eject} parameter, is shown in column 6 of Table 1.

Resonance ejection is typically performed at a fixed q_z value with a fixed supplemental frequency and the mass scan achieved by sweeping the fundamental RF amplitude. For MS/MS applications, various supplemental frequencies are applied as a means of mass isolation, by resonantly ejecting ions of all secular frequencies other than the mass of interest. The trap described herein makes use of frequency scanning of the supplemental waveform to perform the analytical mass scan while maintaining a low but constant fundamental RF voltage and frequency.

Frequency scanning of fundamental waveforms has been performed sparingly by Schlunegger et al. [23] for high mass ions

(up to 150 kDa) and more recently in digital ion traps [24,25] and microparticle [26] and nanoparticle [27] analysis. Scanning a wide range of sinusoidal RF frequencies at moderate amplitudes can be electronically challenging. However, frequency scanning of digital waveforms, pioneered recently by Ding and Kumashiro [24], has been used to analyze masses up to 17 kDa. Typical driving frequencies are maintained from 200 kHz to 1 MHz at voltages from ±250 V to ±1000 V [25]. Unfortunately, the specialized driving circuitry may consume more power than sinusoidal waveforms to achieve such high duty cycle, high voltage digital waveforms. Notably, Wang and Johnston [26] use a commercially available digital pulser driven by a function generator to supply driving frequencies below 150 kHz to analyze nanoparticles. Nie et al. [27] use a home built sinusoidal RF generator at even lower frequencies (<1 kHz) to analyze microparticles. While such low frequencies are suitable for high masses, access to a range of frequencies is desirable to achieve a reasonable dynamic mass range.

In our current configuration, we are able to show an achievable mass range above 1000 Da using frequency scanning of the resonant ejection frequency while maintaining a low amplitude of the fundamental waveform. The clear advantage of such a technique is that the frequency control of the relatively high amplitude fundamental waveform is unnecessary. Precise control of the supplemental waveform frequency with amplitudes no greater than 4 V_{pp} is all that is required. Such a configuration is driven by the need for the simplest of electronic controls aboard a space flight module.

2. Experimental

2.1. Basic design parameters

Commercial trap electrodes, ion optics, and the electron source were removed from a Thermo Electron GCQ Plus mass spectrometer and used inside a home-built vacuum chamber. The trap retained the commercial stretched geometry, that is an r_0 = 0.707 cm and a z_0 = 0.783 cm. It is important to note that this configuration does not comply with the final trap dimensions of MOMA which will make use of an even smaller r_0 of 0.5 cm to extend the mass range. Rather, the readily available commercial hardware was used in this work to demonstrate the concepts of supplemental frequency scanning, mass range extension with low RF voltages, and internal electron ionization. The rhenium filament of the electron filament assembly was powered by an HP1050 constant current power supply (Agilent, Santa Clara, CA). Electron emission was maintained from 1 μA to 10 μA on the electron lens. No means of automatic gain control was employed. Ions were injected by the ion gate lens for 1–10 ms and allowed to cool inside the trap for 30–39 ms before the scan was applied.

A prototype radiofrequency generator from MassTech, Inc. (Columbia, MD) was used to apply a constant RF voltage (50–500 V_{0-p} depending on the scan) to the ring electrode with a frequency of 760 kHz. A Stanford Research Systems (Sunnyvale, CA) Model DS345 Function Generator through a balun transformer (North Hills, Syosset, NY) produced a variable amplitude bipolar frequency sweep to opposite endcap electrodes. No phase coupling was maintained between the fundamental and supplemental RF power supplies. Triggering of each scan was maintained by a Stanford Research Systems (Sunnyvale, CA) DG535 delayed pulse generator, which was also used to control the gates of the electron lens, filament bias, and the ion optics lens. Frequency scan lengths lasted ~270 ms. Amplitude modulation of both the supplemental and fundamental waveform was achieved by a National Instruments (Austin TX) PCI-6221 DAQ card.

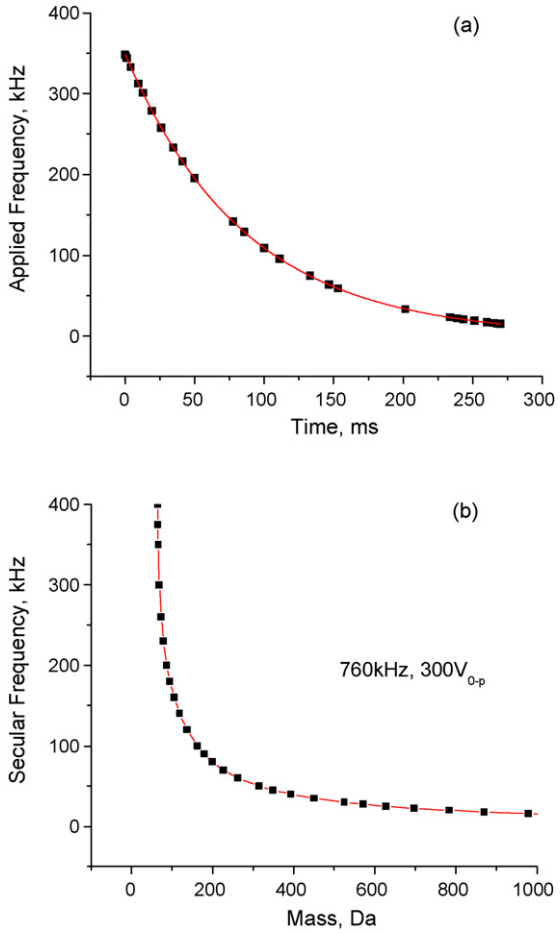

Fig. 1. (a) Applied logarithmic sweep of frequency with time and (b) the theoretical secular frequency as a function of mass.

Microchannel plates from Hamamatsu Corporation (Hamamatsu City, JP) were used for ion detection and operated in a pulse counting mode. Approximately 500 scans were accumulated for each spectrum by a multi-channel scaler (SR430, Stanford Research Systems) and collected through a GPIB connection (National Instruments, Austin, TX) for subsequent processing.

2.2. Calibration and instrument operation

Perfluorotributylamine (PFTBA), a common calibrant for EI mass spectra, was used in most experiments, while Xe isotopes and PSS-octakis(dimethylsyliloxy)-substituted silsesquioxane (Sigma) were used for mass resolution and mass range measurements, respectively. Volatile samples were introduced via a Teflon gas line to the ion source volume through a leak valve (Granville Phillips) with sample pressures typically maintained around 2×10^{-6} Torr. Solid samples were introduced to the external ion source volume with a home-built assembly employing a cartridge heater (Hotwatt, Danvers, MA). Both helium and carbon dioxide were used as buffer gases and maintained at approximately 2×10^{-5} Torr (uncorrected outside of the trap).

Two sweep modes are possible on the DS345 frequency generator, linear and logarithmic in time. Most scans were performed with the logarithmic sweep (Fig. 1a). However, the formula for the fundamental supplemental frequency:

$$\omega_z = \frac{1}{2}\beta_z \Omega \quad (2)$$

and the Dehmelt approximation of the parameter β_z for $q_z < 0.4$

$$\beta_z \approx \sqrt{\frac{1}{2}q_u^2} \tag{3}$$

with Eq. (1), yield the relation

$$\omega \propto \frac{1}{m} \tag{4}$$

suggesting that an inverse frequency sweep in time would simplify the interpretation of the raw mass spectrum. Calculated secular frequencies from ITSIM 5.0 (Aston Labs, Purdue OH) for various masses use a more robust formula for β_z in Fig. 1b for an RF voltage amplitude of 300 V_{0-p}. These points are then used to produce a polynomial fit between frequency and mass. For different RF voltage amplitudes, a different fit must be calculated. The conversion from time to secular frequency (the fit of Fig. 1a) and then from secular frequency to mass (the fit of Fig. 1b) permits the theoretical mass assignments of the frequency scanned spectra. When covering a small range of masses, a linear sweep could suffice. However, to scan a reasonably wide mass range, the practical application of a supplemental frequency sweep would scan the frequency in a non-linear fashion and preferably inversely with respect to time to maintain consistent mass scanning rates. Such an inverse frequency sweep may be performed in the future with an arbitrary waveform generator but was approximated by the logarithmic sweep for the data presented herein.

2.3. External and internal electron ionization modes

The MOMA mass spectrometer is designed to accommodate both an LD and an EI source. While a number of instrumental configurations can be envisioned to satisfy this requirement, one approach is to utilize one of the endcap electrodes as the means to admit ions formed externally by laser desorption and to form ions by electron ionization internally using an electron beam admitted into the ion trap through the ring electrode. Internal ionization by electron impact was utilized in early ion trap mass spectrometers, but was carried out by mounting an electron source on one of the endcap electrodes, which in those instruments were at ground potential. Fig. 2 is a schematic drawing of our current prototype instrument which shows the placement of both the conventional external EI source and an electron source for internal ionization mounted on the ring electrode. The electron source mounted on the ring electrode utilizes a duplicate electron gun assembly identical to that on the external ion source. However, because the ring electrode carries the fundamental frequency during the ionization period some accommodation must be made for biasing the electron source and switching the electron beam on and off. One approach is to float the electron source at the RF voltage to maintain constant electron energy with respect to the ring electrode. The approach used here, however, recognizes the fact that trapping voltages for internal ionization in the mass range for GCMS will be of the order of 100–200 V_{0-p}. The filament is then biased at −60 V (with respect to ground) when the electron beam is turned ON, and +160 V to +240 V when the electron beam is OFF. When turned ON this biasing scheme results in a train of electron beam pulses entering the trap (synchronous with the fundamental RF frequency), but does not appear to adversely affect ionization.

3. Results and discussion

3.1. PFTBA and xenon using external EI source

In our first experiments the external EI source was used, the headspace gas from a PFTBA sample was introduced into the ion source, and ions were injected through the grounded endcap of the trap with a trapping voltage of 300 V_{0-p}. After ~30 ms of cooling, a bipolar 2 V_{pp} waveform was applied to opposite endcaps with the frequency scanned logarithmically from 350 kHz to 15 kHz, representing a mass range from the low mass cut-off (LMCO) limit of 64–1045 Da. Fig. 3(a) shows the raw spectrum of PFTBA, which is then transformed into the frequency spectrum (b) and finally transformed into the mass spectrum (c). The frequency spectrum is measured over the length of the scan and fit with a third-order polynomial. The mass scale is derived from the primary secular frequencies calculated in ITSIM 5.0. The mass spectrum shows the clear mass range extension from 64 Da using a 300 V, 760 kHz RF supply to up to 600 Da by incorporation of the resonance ejection frequency scanning mode.

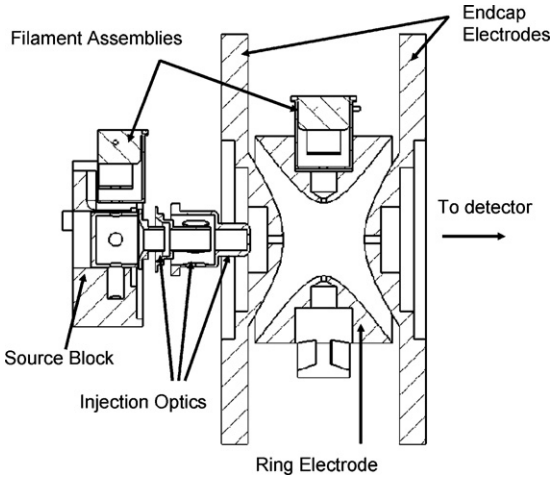

Fig. 2. Schematic diagram of the low voltage ion trap mass spectrometer illustrating the external ionization source and internal ionization using an electron source on the ring electrode. Both means of ionization use identical electron sources consisting of a filament assembly in a cylindrical insert with an exit hole for the electron beam. In the external EI source, the filament is biased at −70 V with respect to the cylindrical insert (and the source block), and the ions are pulsed into the trap using the repeller and ion extraction lenses. In the internal EI mode, the electron beam is pulsed from (typically) −60 V (ON) to +240 V (OFF).

A direct consequence of logarithmically sweeping the supplemental resonance ejection frequency may be seen in the change in resolution across the mass spectrum. As only an approximation to the inverse frequency sweep, the logarithmic sweep still amounts to a non-uniform scan rate. Slow mass scan rates are well known to improve resolution. The fitted polynomial relation of mass over time was derivatized to produce the almost linear increase in mass scan rates shown on the right side of Fig. 3c. Early in the spectrum, the peaks are very tight, owing to the relatively slow mass scan rate but toward the end of the spectrum much faster scan rates prevail indicated by the wide peak widths. For instance, at the peak assignment of m/z 70 with a resolution of ~300, the instantaneous scan rate is 340 Da/s but at m/z 591, the resolution is ~130 and the instantaneous scan rate is approximately 6800 Da/s.

The major peaks of the spectrum were assigned to the characteristic EI spectral peaks of PFTBA, namely masses of 69, 131, 264, 414, 502, and 614 shown in parentheses. For example, the last visible peak, appearing theoretically at 591 Da is presumed to be the m/z 614 peak of PFTBA. Assuming the correct assignment of the peaks, the mass spectrum notably exhibits several dramatic mass "shifts" as noted in Fig. 3. While some small (<1 Da) mass shifting can be owed to space charge and/or buffer gas effects, the extremely large shifts are remarkable in the high mass region reaching up to −23 Da for m/z 614. This can probably be explained by different ejection conditions for ions having different masses (as will be illustrated

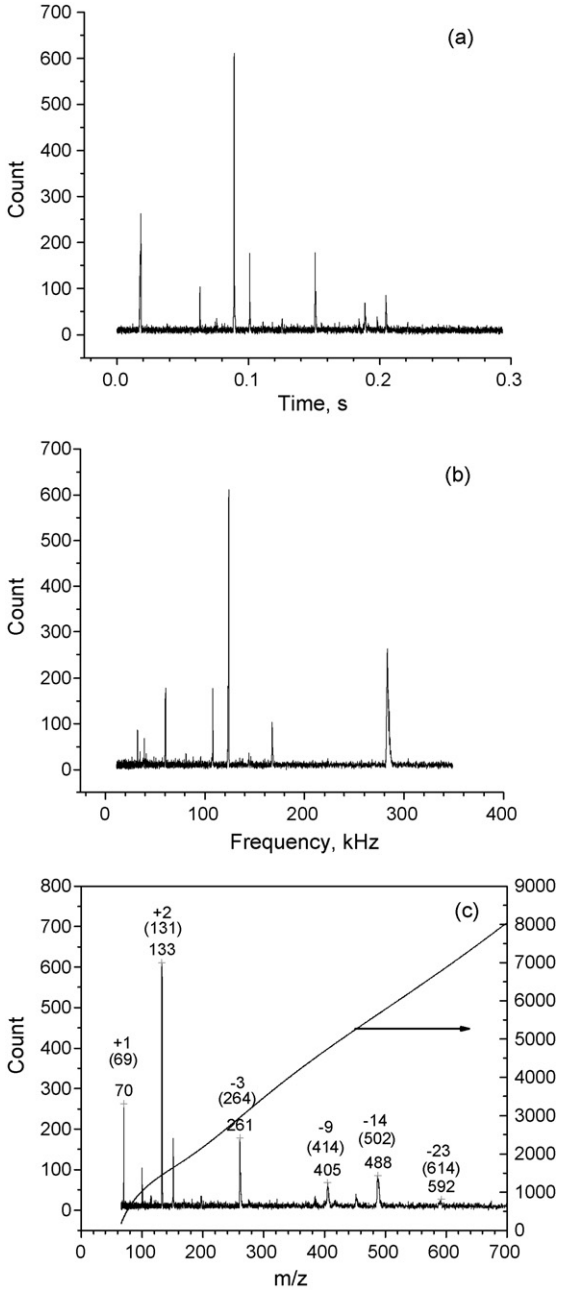

Fig. 3. Mass spectrum of PFTBA: (a) raw spectrum in time, (b) frequency spectrum and (c) theoretical transformed linear scale mass spectrum. The characteristic mass peaks of PFTBA are marked in parentheses above which is provided the mass "shift" based on the theoretical peak assignments. The right axis of plot c shows the corresponding mass scan rate imposed by the logarithmic frequency sweep.

later in Fig. 4). Such a large degree of mass shifting emphasizes the need for calibration standards in practical operation of the frequency scanning mode.

The amplitude of the supplemental waveform is varied in Fig. 4 for PFTBA. Frequencies were scanned logarithmically in time from 375 to 15 kHz, in a "forward" scanning manner from low to high mass, while the fundamental RF voltage is held constant at 151 V_{0-p}. Ions clearly eject earlier at higher frequencies with higher AC amplitudes. This means that the ejection conditions (namely, the amplitude of the supplemental excitation voltage) can affect the ejection time. The "optimal" excitation voltage amplitude should not be very different from the "threshold" value, thus, leaving us

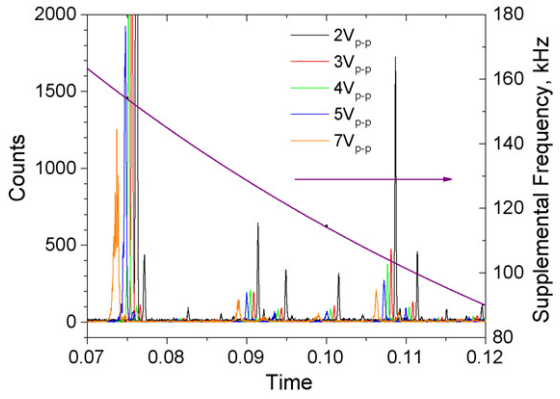

Fig. 4. Mass spectra obtained using a logarithmic scan of the supplemental waveform from 375 kHz to 15 kHz with varying amplitudes of 2, 3, 4, 5 and 7 V_{p-p}. Peaks emerge earlier at higher frequencies with increasing supplemental waveform amplitude.

the room for amplitude optimization in the future. In Fig. 5, the effect of higher order electric fields on the resolution dependence in the forward and reverse scan directions is shown. The raw spectra are shown for both scan directions for a sample of xenon gas. In the forward scan (red), the isotopes of xenon are noticeably distinguishable. The positive octopole component of the commercial configuration causes the ions approaching the endcaps (high amplitude) to increase their secular frequency. The ions thus experience the higher secular frequencies with the decreasing applied supplemental AC frequency, helping to quickly push the ions into resonance in the forward scanning mode. In the reverse scan (black) going from 15 kHz to 350 kHz, a blurred peak denotes the waffling of the ions' secular frequency approaching the endcaps.

The highest observed mass in Fig. 4 is a peak at a frequency of 19.26 kHz, assigned to the 414 Da fragment of PFTBA. Larger peaks including the 614 and 502 Da peaks are conspicuously absent presumably due to the shallow potential energy well depth which complicates trapping. According to the Dehmelt approximation, the pseudopotential well depth of an ion of mass 502 Da is ~1.1 eV ($q = 0.059$), while that of the observed ~414 Da is 1.3 eV ($q = 0.072$). Such shallow well depths prove to be a limiting factor as it decreases with higher mass. Unlike the frequency scans of Ding et al. [25] in which the instability point remains constant across the scan, maintaining a single potential well depth, our configuration scans the

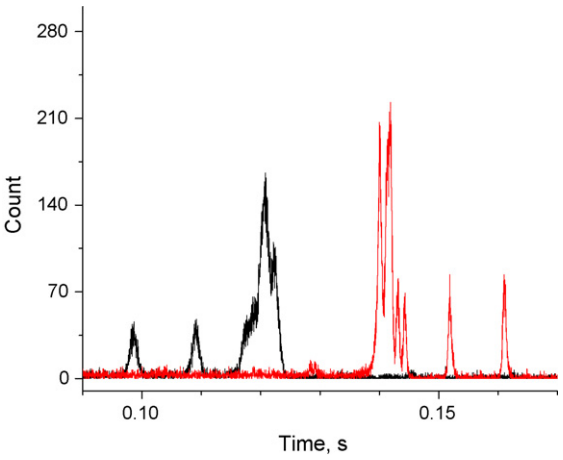

Fig. 5. A forward (red) and reverse (black) scans show a marked difference in resolution for a sample of xenon gas. The isotopes of xenon are clearly visible in the forward scan which benefits from non-linear effects.

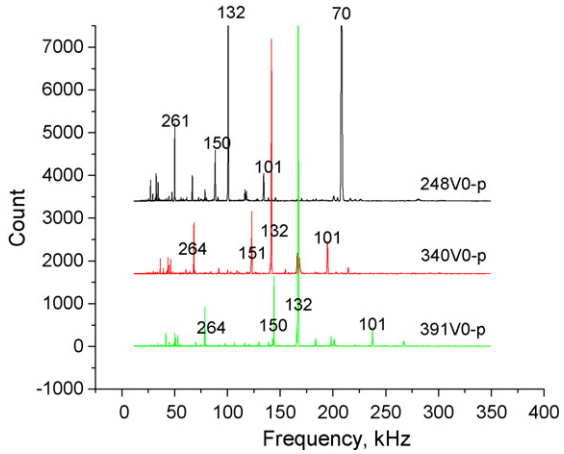

Fig. 6. The fundamental RF trapping voltage is adjusted to 248 V_{p-p} (black), 341 V_{p-p} (red), and 391 V_{p-p} (green).

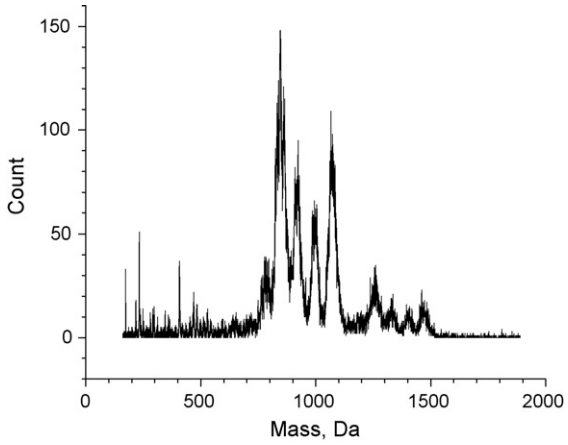

Fig. 8. EI mass spectrum of PSS-octakis(dimethylsyliloxy)-substituted silsesquioxane in the region of m/z 1000.

instability point and thus the potential well depth is not constant across all masses. However, such a calculation does provide some insight on the limitation of resonance ejection to extend our mass range.

To increase the well depth for higher masses (lower q), we may raise the trapping voltage. In Fig. 6, the consequence of using higher trapping voltages is a higher low mass cut-off as evidenced by the loss of the ~69 m/z peak at voltages above 248 V_{0-p}. The higher trapping voltages do not result in noticeably increased high mass sensitivity though this may simply reflect the relatively low intensity of the high mass region of PFTBA. An optimization of the operating mass modes (by varied trapping voltage) must balance high mass sensitivity with the low mass cut-off.

In Fig. 5, the relatively poor resolution of even the forward scanned spectrum is achieved with a scan rate of approximately 1400 Da/s, already four times slower than the commercial scan rates of ~5000 Da/s. Even slower scan rates were employed to demonstrate the capacity for enhanced resolution in Fig. 7. Some moderate gains in resolution were achieved with scan rates 1000, 500, and 250 Da/s by simply increasing the length of the scan. The isotopes 131 and 132 are baseline resolved in the slowest scan. We believe further improvements in the resolution may be accomplished with a more stable fundamental RF power supply. Instability in the amplitude of the fundamental RF power supply employed have been observed as high as 6 V_{p-p} which for high q values like the instability boundary of 0.908 evokes a mass assignment error of ~0.7 Da but at a q value as low as 0.2, produces an error of 3 Da. Notably, the commercial RF power supply used was originally developed for simpler quadrupole mass filter applications.

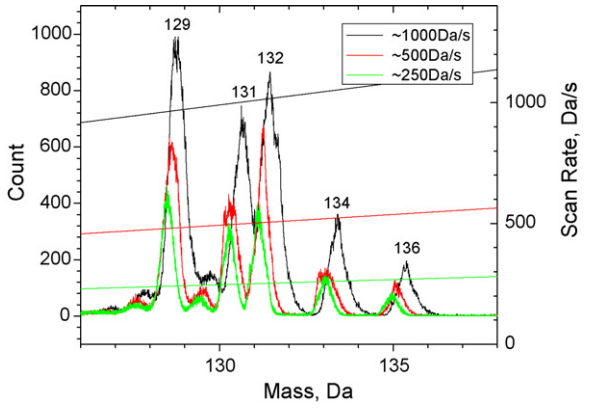

Fig. 7. A series of slow scans is performed with the resulting mass spectra for scan rates of ~1000 Da/s (black), ~500 Da/s (red), and 250 Da/s (green) by doubling and then quadrupling the scan duration.

3.2. Higher mass ranges

PSS-octakis(dimethylsyliloxy)-substituted silsesquioxane, a higher mass compound (MW 1017) which is mildly volatile at room temperature, was chosen for the relative large high mass to low mass ion abundance in its EI spectrum to examine higher mass ranges. In this case, a fundamental RF amplitude of 300 V_{0-p} was used on the ring electrode, while the supplemental RF on the endcaps of 4 V_{p-p} was scanned logarithmically from 100 KHz to 10 KHz. Solid sample was desorbed from a heater at ~52 °C directly into the external EI source, and its mass spectrum recorded as in Fig. 8. Such an observation shows a promising mass range extension using q values as low as 0.037.

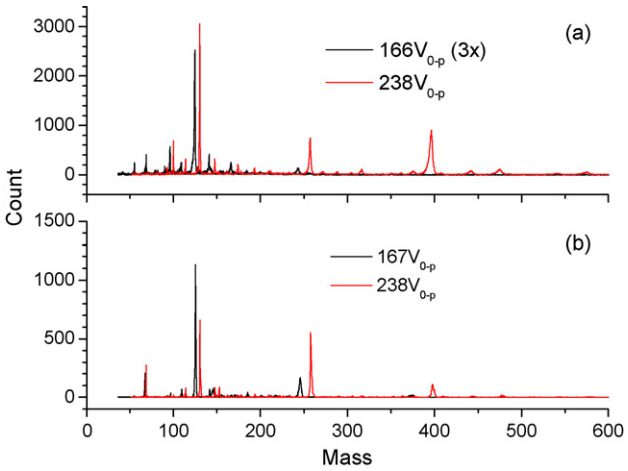

Fig. 9. Mass spectra with CO_2 as the bath gas. (a) Internal ionization using an electron source mounted on the ring electrode, and (b) electron ionization in an external source. In plot a demonstrating the use of internal ionization, the black trace employs an "OFF" bias of +160 V for the 166 V_{0-p} fundamental RF amplitude while the red trace employs an "off" bias of +240 V for a 238 V_{0-p} fundamental RF amplitude. The black and red traces in plot (b) demonstrate the corresponding fundamental RF amplitudes 166 V_{0-p} and 238 V_{0-p} (respectively) used for the external ionization mode.

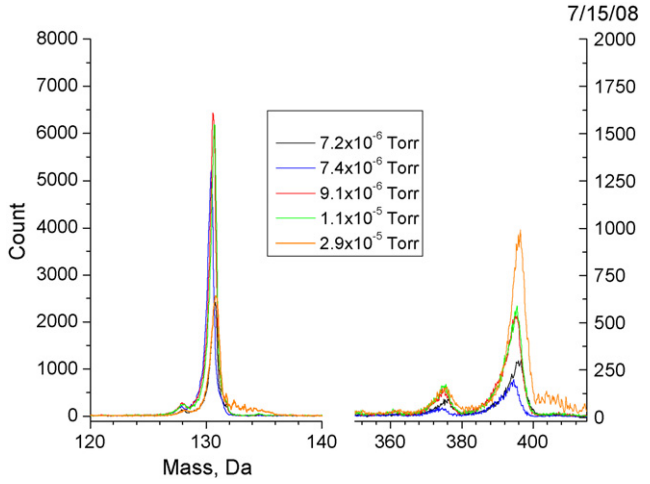

Fig. 10. Concentration study of CO_2 as bath gas on the internal EI signal of PFTBA.

3.3. Internal electron ionization through the ring electrode with CO_2 as the bath gas

This prototype enabled us to develop the capability for internal ionization using an electron beam entering through the ring electrode and to test the possibility for using carbon dioxide (the major constituent of the Mars atmosphere) as a bath gas for cooling and trapping the ions. Fig. 9 compares spectra of PFTBA obtained with the internal and external EI sources using CO_2 as the bath gas. In the internal ionization mode shown in Fig. 9(a), the filament "Off" bias condition is set to be approximately consistent with the trapping voltage amplitude. Thus, the red trace of plot (a) shows the mass spectra with trapping voltage at 237.5 V_{0-p} and the ON/OFF bias set at −60/+240 V. In the black trace of (a) the trapping voltage is reduced to 166.5 V_{0-p} and the filament ON/OFF bias to −60/+160 V. In this case, the higher mass ion signal is reduced while the low mass cut-off is also reduced to include ions at the low mass end of the spectrum. In the external ionization mode in Fig. 9(b) similar results are observed at trapping voltages of 166.5 V_{0-p} and 237.5 V_{0-p} in the black and red traces, respectively. Many of the major mass peaks are observed in both external and internal configurations using CO_2. Some additional peaks in the case of internal ionization may be related to the ionization of CO_2 itself inside the trap at least in the case of the sample of perfluorotributylamine. As expected, the internal ionization method results in better overall signal intensities.

The pressure of CO_2 inside the ion trap, when used as the bath gas, cannot be directly determined in our instrument. We therefore performed a series of experiments in which the CO_2 pressure was varied and measured in the vacuum chamber outside the ion trap. As shown in Fig. 10 the pressure ranged from 7.2×10^{-6} Torr to 2.9×10^{-5} Torr. In general, higher CO_2 pressures showed an increase in the intensity of the ion signal at m/z 414 relative to the signal at m/z 131.

4. Conclusions

The constraints of size, weight and power for the upcoming Mars mission dictated the need for the development of a compact instrument operated at low voltage and low RF power. In this case miniaturization is not the goal, the ability to record masses in a range that might suggest the existence of organic or biological molecules is. In the current prototype we have been able to show that the use of a supplemental RF frequency on the endcaps can extend the mass range on a 300 V instrument just as it does on higher voltage (generally 7.5 kV_{0-p}) instruments. The choice of 300 V as the fundamental RF amplitude in this case reflects the 300 volts used earlier in the Rosetta mission [21] where a mass range of 150 was achieved using the *mass selective instability* mode only. Scanning the supplementary frequency (rather than the fundamental RF amplitude) also helps to reduce the need for high voltage and power, as ions can be ejected at voltages just sufficient to trap the ions. Supplemental frequency scanning also decouples the power–mass range relationship by obviating the need for precise amplitude control of a high voltage RF. While different mass scanning modes are anticipated, the electronics are still greatly simplified requiring only precise frequency control of the low voltage waveforms. In addition, a novel design that enables input of the electron beam through the ring electrode offers the practical possibility of incorporating up to four redundant filaments. We do note that one disadvantage of an internal source is the potential build up of contamination from the effluent flow of the gas chromatograph. However, the limited number of GC runs that are planned in this scenario limit the extent of contamination anticipated. Furthermore, calibrations are expected to be performed at frequent intervals to account for mass shift complications. While our current prototype makes use of an $r_0 = 0.707$ cm geometry, future work will include the use of a trap with smaller radius (0.5 cm) to further extend the mass range up to 2000 Da and enable the detection of "high" mass organics on Mars as part of the scientific payload of ExoMars. Should these high mass organics be detected, the question of life on Mars could soon be addressed.

Acknowledgements

This work was supported by the NASA-ASTEP program contract NNH07ZDA001N (L. Becker) and NASA TDP program contract NNG08GGB7G (L. Becker). The authors thank the Cooks group for the generous use of their ITSIM software for calculations of the ions' secular frequencies.

References

[1] D.M. Anderson, K. Biemann, L.E. Orgel, J. Oro, T. Owen, G.P. Shulman, P. Toulmin III, H.C. Urey, Icarus 16 (1972) 111.
[2] D.R. Rushneck, A.V. Diaz, D.W. Howarth, J. Rampacek, K.W. Olson, W.D. Dencker, P. Smith, L. McDavid, A. Tomassian, M. Harris, K. Bulota, K. Biemann, A.L. LaFleur, J.E. Biller, T. Owen, Rev. Sci. Instrum. 49 (1978) 817.
[3] P.T. Palmer, T.F. Limero, J. Am. Soc. Mass Spec. 12 (2001) 656.
[4] J.H. Waite Jr., M.R. Combi, W.-H. Ip, T.E. Cravens, R.L. McNutt Jr., W. Kasprzak, R. Yelle, J. Luhmann, H. Niemann, D. Gell, B. Magee, G. Fletcher, J. Lunine, W.-L. Tseng, Science 311 (2006) 1419.
[5] H.B. Niemann, S.K. Atreya, G.R. Carignan, T.M. Donahue, J.A. Haberman, D.N. Harpold, R.E. Hartle, D.M. Hunten, W.T. Kasprzak, P.R. Mahaffy, T.C. Owen, N.W. Spencer, S.H. Way, Science 272 (1996) 846.
[6] K. Biemann, J. Oro, P. Toulmin III, L.E. Orgel, A.O. Nier, D.M. Anderson, P.G. Simmonds, D. Flory, A.V. Diaz, D.R. Rushneck, J.E. Biller, J. Geophys. Res. 82 (1977) 4641.
[7] G.A. Soffen, J. Geophys. Res. 82 (1977) 3959.
[8] K. Biemann, Proc. Natl. Acad. Sci. 104 (2007) 10310.
[9] K. Biemann, J. Mol. Evol. 14 (1979) 65.
[10] L. Becker, B. Popp, T. Rust, J.L. Bada, Sci. Lett. 167 (1999) 71.
[11] R.A. Kerr, Science 320 (2008) 738.
[12] D. Meunier, R. Sternberg, F. Mettetal, A. Buch, D. Coscia, C. Szopa, C. Rodier, P. Coll, M. Cabanec, F. Raulin, Adv. Space Res. 39 (2007) 337.
[13] W.L. Davis, C.P. McKay, Origins Life Evol. Biospheres 26 (1996) 61.
[14] J.L. Bada, D.P. Glavin, G.D. McDonald, L. Becker, Science 279 (1998) 362.
[15] L. Becker, D.P. Glavin, J.L. Bada, Geochim. Cosmochim. Acta 61 (1997) 475.
[16] D.S. McKay, E.K. Gibson Jr., K.L. Thomas-Keprta, H. Vali, C.S. Romanek, S.J. Clemett, X.D.F. Chillier, C.R. Maechling, R.N. Zare, Science 273 (1996) 924.
[17] F. Goesmann, H. Rosenbauer, R. Roll, C. Szopa, F. Raulin, R. Sternberg, G. Israel, U. Meierhenrich, W. Thiemann, G. Munoz-Caro, Space Sci. Rev. 128 (2007) 257.
[18] J.F.J. Todd, S.J. Barber, I.P. Wright, G.H. Morgan, A.D. Morse, S. Sheridan, M.R. Leese, J. Maynard, S.T. Evans, C.T. Pillinger, D.L. Drummond, S.C. Heys, S.E. Huq,

B.J. Kent, E.C. Sawyer, M.S. Whalley, N.R. Waltham, J. Mass Spectrom. 42 (2007) 1.
[19] L. Gao, Q. Song, G.E. Patterson, R.G. Cooks, Z. Ouyang, Anal. Chem. 78 (2006) 5994.
[20] R.E. Kaiser Jr., R.G. Cooks, J. Moss, P.H. Hemberger, Rapid Commun. Mass Spectrom. 3 (2) (1989) 50.
[21] R.E. March, J.F.J. Todd, in: J.D. Winefordner (Ed.), Chemical Analysis, 165, 2nd ed., John Wiley & Sons, Inc., Hoboken, NJ, 2005.
[22] J.M. Wells, E.R. Badman, R.G. Cooks, Anal. Chem. 70 (1998) 438.
[23] U.P. Schlunegger, M. Stoeckli, R.M. Caprioli, Rapid Commun. Mass Spectrom. 13 (1999) 1792.
[24] L. Ding, S. Kumashiro, Rapid Commun. Mass Spectrom. 20 (2006) 3.
[25] L. Ding, M. Sudakov, F.L. Brancia, R. Giles, S. Kumashiro, J. Mass Spectrom. 39 (2004) 471.
[26] S.Y. Wang, M.V. Johnston, Int. J. Mass Spectrom. 258 (2008) 50.
[27] Z. Nie, F. Cui, M. Chu, C.-H. Chen, H.-C. Chang, Y. Cai, Int. J. Mass Spectrom. 270 (2008) 8.